

# Application of Nuclear Microprobe in Biomedical, Industrial and Fusion Research

P. Vavpetič, N. Grlj, P. Pelicon,

Jožef Stefan Institute, Association EURATOM-MHEST, Jamova 39, SI-1000, Ljubljana, Slovenia

Email contact of main main author: primoz.vavpetic@ijs.si

**Abstract.** Nuclear microprobe at 2 MV Tandetron accelerator of Jozef Stefan Institute (JSI) was constructed in the year 2000 with the support of IAEA Technical Cooperation Project SLO/1/004. The measuring station is equipped with instrumentation for micro-Proton-Induced-X-ray-Emission (micro-PIXE), micro-Elastic Recoil Detection Analysis (micro-ERDA), micro-Nuclear Reaction Analysis (micro-NRA), Proton Beam Writing (PBW) and confocal PIXE.

Micro-PIXE elemental mapping in biomedical research has been established as routine analytical method at JSI tandetron laboratory for collaborators from biomedical fields. Research results from the last two years include, among others, elemental distribution in the leaves and seed of Cd/Zn hyperaccumulating plant *Thlaspi Praecox* grown in heavy-metal polluted area, leaves of halophyte plants, elemental distribution of buckwheat seed, elemental contents of wood, lichen arsenate uptake etc. From analytical point of view, some results of elemental mapping measured at an interesting example of brain tissue of mercury miner sampled for pathological depot over a decade ago and recently retrieved for Hg/Se analysis will be presented.

On the other hand, the intensifying research associated with the construction of the future thermonuclear reactor ITER is expressing in the development of the techniques for detection of hydrogen isotopes in the tokamak wall materials. Hydrogen microdistribution in the exposed tokamak wall materials are measured by micro-ERDA using focused 3 MeV  ${}^7\text{Li}$  beam. Post-mortem micro-ERDA analyses of tokamak plasma-exposed surfaces were combined with simultaneous X-ray emission to understand erosion-redeposition processes in the tokamak walls. Micro-ERDA has been also recently used for determination of hydrogen concentrations in titanium alloys for industrial customers. In addition, micro-NRA for deuterium mapping has been established with  ${}^3\text{He}$  beam using nuclear reaction  $\text{D}({}^3\text{He},\text{p}){}^4\text{He}$ . Carbon fiber composites, the candidate materials for the ITER divertor, were exposed to the deuterium plasma inside tokamak Textor. Deuterium penetration depth was then determined by micro-NRA.

## 1. Introduction

Proton-Induced X-ray Emission spectroscopy (PIXE) is analytical method, based on the X-ray excitation of fast protons in the sample. Its high elemental sensitivity is result of low physical background in PIXE spectra, consisting of primary proton bremsstrahlung and bremsstrahlung of secondary electrons [1] (Ishii et al., 2005). It is mostly used for the measurements of trace elements composition in various types of materials. The limits of detection range from 0.1 to 1  $\mu\text{g g}^{-1}$  (ppm) for mid-Z elements ( $20 < Z < 40$ ) and generally well below 10 ppm elsewhere for the elements ranging from Na to U [2] (Johansson and Campbell, 1988). Applications of standard PIXE method, where a proton beam with diameter of several millimeter is used to induce X-rays in the sample, extends from geology, archaeometry, air aerosol particulate studies to the homogenized biological materials.

## 2. Micro-PIXE

The capability of the PIXE technique is largely extended in the case of its application with focused proton beam. High energy focused proton beam setups are frequently referred to as nuclear microprobes [3] (Breese, 1996). Ion lenses are able to focus the beam down to the sub-micrometer diameter. By scanning of the focused proton beam in raster mode and by

detection of induced X-rays, lateral elemental distribution maps within the samples are measured. The acronym of the method is micro-PIXE.

### **2.1. Micro-PIXE in Biomedical Research**

Proton-Induced X-ray Emission spectroscopy with focused proton beam, frequently referred to as micro-PIXE, has long been known as an efficient technique to measure lateral elemental distribution within thin biological tissue sections. In combination with Scanning Transmission Ion Microscopy (STIM), which provides lateral thickness distribution of the sample, it enables quantitative elemental mapping of biological tissue. For intermediate thickness samples the thickness of the tissue section could be accurately preset on the microtome. During the cutting, the tissue is frozen and contains its normal water content. Freeze-drying resulted in an uneven thickness of the specimen due to a variation of the morphological structure over the section of the specimen. Absolute concentrations in the fresh tissue could be conveniently provided to the bio-medical community of users. This approach does not require an assumption of even matrix area distribution over the specimen in order to provide useful absolute concentrations of elements.

The main advantage of instrumentally demanding micro-PIXE in comparison with comparable methods, such as frequently available energy dispersive X-ray micro analysis (EDXMA) available at scanning electron microscopes (SEM), is its superior sensitivity. In general, micro-PIXE features approximately two orders of magnitude higher elemental sensitivity than EDXMA [4] (Legge and Cholewa, 1994). As the reliability of required instrumentation, which includes accelerator, microbeam forming system and detectors, significantly improved in the last decade, the method is becoming readily available to the external users in several laboratories upon scientific proposal as standard technique for quantitative elemental mapping in biological tissue.

Key starting point in micro-PIXE analysis on biological materials is sample preparation. Over the last two decades, a procedure consisting of tissue cryo-fixation, slicing and freeze-drying is most frequently used for biological tissue containing large quantity of water. The method turned to provide excellent results on the elemental distribution on the tissue and single cell level. However, when the elemental image of sub-cellular structures is concerned, the absence of water results in inner-cell morphology deformation, including shrinking of the cellular wall and membrane, sticking of cellular internal structures to the walls. Advanced possibility of sample preparation without freeze-drying is to keep the tissue frozen after cryofixation and during the analysis. This method of tissue preparation is the most promising direction for tissue treatment at the new generation of nuclear nanoprobe, where PIXE is expected to be available with sub-500 nanometer beam. In the same time, it is the sample preparation technique of choice for the 3D X-ray imaging methods at nuclear microprobes emerging from STIM-PIXE [5] (Habchi et al, 2006) or 3D PIXE with confocal capillary setup [6] (Karydas et al, 2007). Cold in-vacuum manipulator is under construction at Jožef Stefan Institute for micro-PIXE on frozen hydrated tissue.

### **2.2. Micro-PIXE setup at JSI**

Detection of X-ray energies from 1 keV up to 25 keV is enabled by a pair of X-ray detectors. A high-purity germanium X-ray detector with an active area of 95 mm<sup>2</sup>, 25 μm-thick beryllium window and 100 μm thick polyimide absorber is positioned at an angle of 135° with respect to the beam direction. Simultaneously, a Si(Li) detector with an area of 10 mm<sup>2</sup> is installed at the angle of 125° with respect to the beam direction for detection of low energy X-rays in the energy range from 0.8 keV to 4 keV.

### 2.3. Proton flux measurement

Quantitative micro-PIXE analysis can only be done by precise proton dose determination. Ion beam charge integration, which is used for broad-beam PIXE measurements, may introduce large errors in the quantification procedure due to low current, charge exchange between the beam and the sample, secondary electron escaping the sample etc. [7] (ElBouanani et al., 2005). For this reason, in-beam chopping device is positioned in the beam line between the collimation slits and quadrupole triplet lens. The rotating chopper consists of a gold-coated graphite and periodically intersects the beam with a frequency of approx. 10 Hz, which makes the method insensitive to beam intensity fluctuations. Spectrum of backscattered protons from the chopper is recorded in parallel with PIXE spectra in a list mode. High-energy part of the spectrum consists of protons scattered from Au layer and appears as a separate peak. Its area is proportional to the proton flux. During the off-line data processing, the spectrum accumulated at the chopper over an arbitrary scanning area could be extracted from the list-mode data simultaneously with PIXE spectra.

### 2.4. Measurement Sequence

High and low current modes are applied sequentially at the same sample region of interest for the analysis of thin biological samples at the nuclear microprobe of Jožef Stefan Institute [8, 9] (Simčič et al. 2002; Pelicon et al. 2005). In a high-current mode used for micro-PIXE analysis, proton beam with energy of 3 MeV with a diameter varying from 1 to 3  $\mu\text{m}$  at ion currents ranging from 40 to 700 pA is formed, depending on the required lateral resolution. In the low energy mode, object slits are closed to reduce the beam flux to app. 500 protons per second. In this case the silicon charge particle detector is positioned directly in the beam to obtain best contrast in the Scanning Transmission Ion Microscopy (STIM), which is used for determination of specimen thickness. Thickness of the sample in the selected area is extracted from the STIM spectrum and loaded as the beam exit energy in GupixWin [10] program.

The regions of interest at the samples are pre-selected by a short PIXE mapping. After final sample positioning and scan size selection, the object slits are closed to obtain low current beam with flux of about 500 protons per second. Zero-degree STIM maps are measured in a list mode. In a second step, high-current mode is applied by opening the object slits and PIXE maps of the same region are measured in a list mode over a longer periods. As a third and the last step, a “post-mortem” STIM map is again measured at the same area in a list mode to check for sample consistency, thinning and eventual shrinking.

After encouraging results with on-off axis STIM, first reported by the Lund group [11], a similar setup was constructed at JSI, which will enable STIM measurement of distinct quality in parallel with micro-PIXE, without a need for the instrumentally and time-demanding sequential transfer of the setup in the low-current and back to high current mode.

## 3. Formation of $^3\text{He}$ High Energy Focused Ion Beam at Tandem Ion Accelerator

The formation of the accelerated helium ion beam at the injector of tandem accelerators is demanding in comparison with other ion beams. The negative ion beam, required for the injection in the accelerating column of a tandem accelerator, could be extracted directly with a negative charge, either from plasma or from a solid material bombarded by cesium ions [12] (Ion cookbook). Negative helium ion is, however, metastable, with low binding energy of the third electron. The lifetime of  $\text{He}^-$  triplet state ions, which represent approx. half of the ions, is 9 microseconds. The lifetime of other half in a singlet state is 340 microseconds [13] (Wolf et al. 1999). The only known approach to produce negative He beams of considerable

intensity is a two-step process consisting of positive ion extraction and charge exchange in alkali vapors. As accelerated He ions traditionally play important role in research with accelerated ions, the two-step process is implemented in commercially available ion sources for He<sup>-</sup> ions. In comparison with single-ended accelerators, where positive extraction of helium ions is straightforward and results in high brightness of the beam, negative <sup>3</sup>He ion beam is required for tandem accelerator.

### 3.1. <sup>3</sup>He High Energy Focused Ion Beam at JSI

In the tandem accelerator facility at JSI, a positive <sup>3</sup>He beam is extracted from duoplasmatron and directed in a lithium charge exchange canal. Injecting currents of up to 2 μA of <sup>3</sup>He<sup>-</sup> beam are obtained, with sustainable long-running configuration featured currents of approximately 400 nA. The resulting microbeam of approx. 5 x 5 μm<sup>2</sup> with currents of the order of 200 pA is achieved. Ion beam optics parameters for the microbeam formation are calculated within the first order matrix calculation and agree well with the manual beam transmission optimization.

Detection of high energy protons with energy of 10-12 MeV originating from the D(<sup>3</sup>He,p)<sup>4</sup>He reaction is performed by silicon detector employing 0.5 mm absorber. In this way, the reaction products from (<sup>3</sup>He,p) reactions on other light elements, such as carbon, beryllium and oxygen, is completely suppressed and the energy spectrum detected consists of single peak.

### 3.2. Fusion-related Research at JSI

Revival of the fusion-related research in the last years is largely propelled by the decision for the construction of ITER, the tokamak-type thermonuclear reactor employing deuterium-tritium reaction [14] (IterHomepage). Among numerous technological problems connected with the construction of ITER inner walls, the retained tritium in its walls is one of important concerns.

The evaluation of retention processes in wall materials rely mostly on deuterium quantification in the tokamak plasma-exposed wall materials, since hydrogen (<sup>1</sup>H) may be additionally introduced in the form of moisture during sample atmospheric exposure and tritium handling imposes severe safety measures. Several available analytical techniques for deuterium detection provide distribution information with a lateral resolution of typically 1 mm<sup>2</sup>. Deuterium detection techniques with high-energy focused ion beam include Elastic Recoil Detection Analysis (ERDA) and Nuclear Reaction Analysis (NRA) with <sup>3</sup>He microbeam employing D(<sup>3</sup>He,p)<sup>4</sup>He reaction.

In order to understand fuel retention processes, position-sensitive methods able to detect deuterium with high lateral resolution are sought for, as the retained fuel in the wall materials exhibit non-uniform lateral distribution. Mean surface roughness exceeding 10 micrometers is inherent to many objects of interest retrieved from tokamak reactors. These include cleaved bulk wall samples of wall candidate materials for the ITER walls and even the surface of Carbon Fibre Composites (CFCs) selected for construction of ITER divertor. With larger depth range and perpendicular beam impact applied, the NRA employing D(<sup>3</sup>He,p)<sup>4</sup>He reaction is less sensitive on the roughness in comparison with ERDA. Taking into account larger depth range of NRA, it is preferred choice for post-mortem analysis of objects exposed to tokamak plasma.

#### 4. Research Results and Discussion

Hypophysis and kidney tissue of the miner working all his working period in mercury mine without any pathological symptoms was sliced, pathologically examined and stored in a depot. Years later, more info was sought for the tissue elemental composition. Micro-PIXE analysis showed that kidney tissue did not show any Hg contamination (concentration bellow L.O.D of 10 ppm). Hypophysis, however, showed high concentration of Hg of over 200 ppm (see Fig. 1). Measured Se and Hg concentrations of 90 ppm and 229 ppm, respectively, result in stoichiometry ratio of app. 1:1. Selenium probably play a significant role in Hg toxicity deactivation (in collaboration with I. Falnoga).

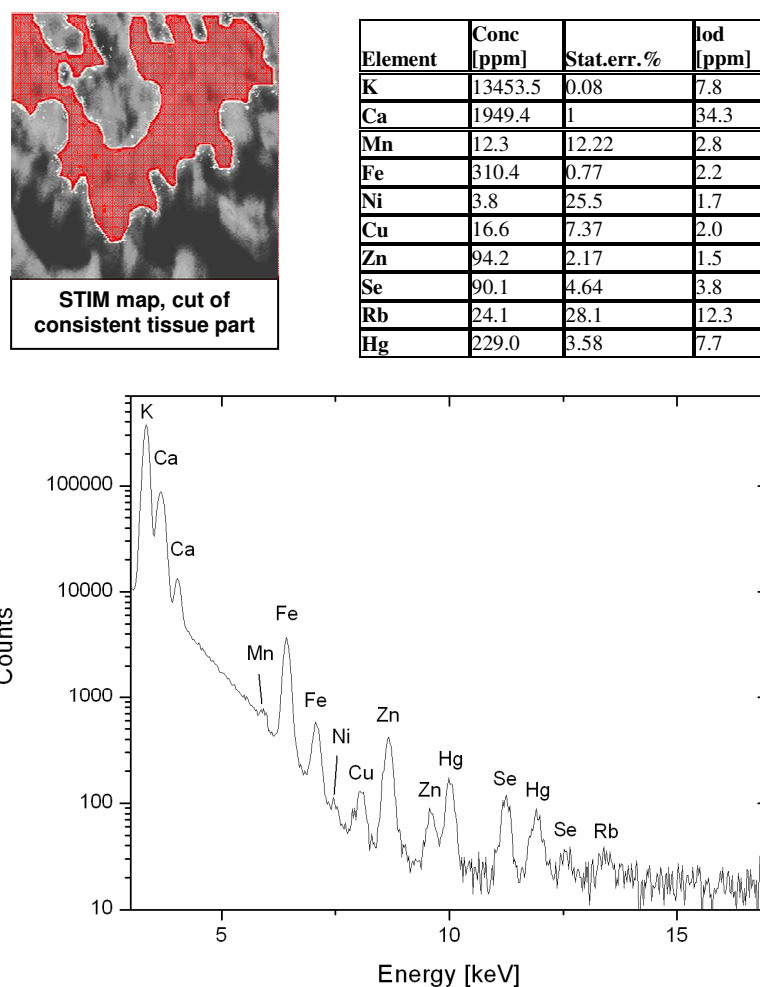


Fig. 1. STIM map (top left), cut of consistent tissue part with red marked area for analysis with corresponding table of concentrations (top right) and recorded spectrum from Germanium detector (bottom).

Hydrogen microdistribution in the exposed tokamak wall materials are measured by micro-ERDA using focused 3 MeV  $^7\text{Li}$  beam. Post-mortem micro-ERDA analyses of tokamak plasma-exposed surfaces were combined with simultaneous X-ray emission to understand erosion-redeposition processes in the tokamak walls.

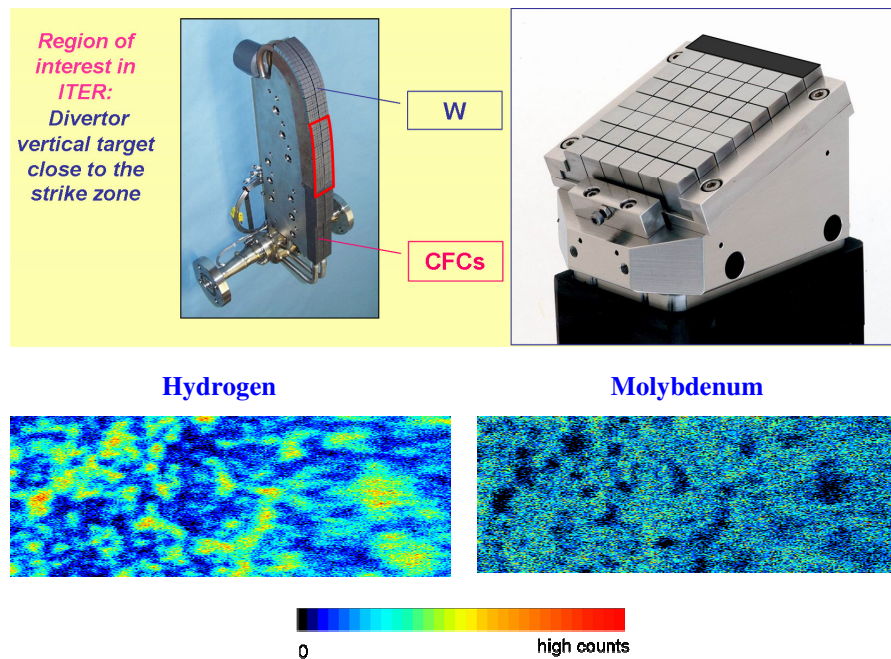


Fig. 2. Areal distribution of hydrogen and molybdenum measured simultaneously by ERDA and Li-beam excited X-ray emission (LIXE) over an area of  $1240 \times 450 \mu\text{m}^2$  (bottom). The surface belongs to a graphite section of the castellation limiter (top), studied in the work of Litnowski et al. [15], exposed inside the plasma of TEXTOR tokamak, IPP Juelich. Molybdenum originates from re-deposition process from neighbour castellation sections made of molybdenum. Hydrogen and molybdenum surface concentrations are anti-correlated.

## 5. Conclusion

High-energy focused ion beam at Jožef Stefan tandemron accelerator is a multi-technique measuring setup, which is enabling interdisciplinary research at the field of biomedicine, material science and fusion. Development of new experimental techniques takes place at the set-up, including confocal PIXE and micro-PIXE on frozen hydrated tissue.

## 6. Acknowledgement

The work is supported by the research project J7-0352 and research program P1-0112 of Slovenian Research Agency (ARRS). Support of fusion research within Association Euratom-MHEST is acknowledged. Accelerator facility is funded by ARRS as Infrastructure Research Centre. Accelerator facility and microprobe were built with substantial support of IAEA in the frame of TCP SLO/1/003 and TCP SLO/1/004.

## 7. References

- [1] K. Ishii K., Yamazaki H. , Matsuyama S. , Galster W., Satoh T., Budnar M. (2005), Contribution of atomic bremsstrahlung in PIXE spectra and screening effect in atomic bremsstrahlung, *X-Ray Spectrometry* 34, 363 – 365.
- [2] Johansson S. A. E. , Campbell J. L. (1988), *PIXE: A novel technique for elemental analysis*. John Wiley & Sons, New York (1988).
- [3] Breese, M. B. H., Jamieson D.N., King, P. J. C. (1996), *Materials Analysis Using a Nuclear Microprobe*. John Wiley & Sons, New York.
- [4] Legge G.J.F. , Cholewa M. (1994). The principles of proton probe microanalysis in biology. *Scanning Microscopy Supplement* 8, 295-315.
- [5] Habchi C., Nguyen D.T., Devès G., Incerti S., Lemelle L., Le Van Vang P., Moretto Ph., Ortega R., Seznec H., Sakellariou A., Sergeant C., Simionovici A., Ynsa M.D., Gontier E., Heiss M., Pouthier T., Boudou A., Rebillat F. (2006), Three-dimensional densitometry imaging of diatom cells using STIM tomography. *Nuclear Instruments and Methods in Physics Research B* 249, 653-659.
- [6] Karydas A.-G., Sokaras D., Zarkadas C., Grlj N., Pelicon P., Žitnik M., Schütz R., Malzer W., Kanngießer B. (2007), 3D Micro PIXE—a new technique for depth-resolved elemental analysis, *Journal of Analytical Atomic Spectrometry* 22, 1260 – 1265.
- [7] M. El Bouanani, P. Pelicon, A. Razpet, I. Čadež, M. Budnar, J. Simčič and S. Markelj Simple and accurate spectra normalization in ion beam analysis using a transmission mesh-based charge integration. *Nucl. Instr. and Meth. B* 243 (2006) 392-396
- [8] J. Simčič, P. Pelicon, M. Budnar, Ž. Šmit, The performance of the Ljubljana ion microprobe. *Nucl. Instr. and Meth. B* 190 (2002) 283.
- [9] P. Pelicon, J. Simčič, M. Jakšič, Z. Medunić, F. Naab, F.D. McDaniel, Spherical chamber-effective solution for multipurpose nuclear microprobe. *Nucl. Instr. and Meth. B* 231 (2005) 53.
- [10] Campbell J.L., Hopman T.L., Maxwell J.A. & Nejedly Z. (2000) The Guelph PIXE software package III: Alternative proton database. *Nuclear Instruments and Methods in Physics Research B* 170, 193-204.
- [11] Pallon J., Auzelyte V., Elfman M., Garmer M., Kristiansson P., Malmqvist K., Nilsson C., Shariff A. and Wegdén M. (2004), An off-axis STIM procedure for precise mass determination and imaging, *Nuclear Instruments and Methods in Physics Research B* 219-220, 988-993.
- [12] *A Negative Ion Cookbook* by Roy Middleton, 1989
- [13] Wolf A, Bhushan KG, Ben-Itzhak I, Altstein N, Zajfman D, Heber O, Rappaport ML, *Phys. Rev. A* 59 (1999), 267.
- [14] <http://www.iter.org/index.htm>
- [15] A. Litnovsky, V. Philipps, P. Wienhold, G. Sergienko, B. Emoth, M. Rubel, U. Breuer, E. Wessel, *J. Nucl. Mater.* 337-339, 917 (2005).